

EXPERIMENTAL CREEP STUDY OF METALS UNDER MULTIAXIAL STRESS CONDITIONS

ZBIGNIEW L. KOWALEWSKI

Institute of Fundamental Technological Research, Warsaw

e-mail: zkowalew@ippt.gov.pl

Theoretical and experimental methods of creep analysis of metals subjected to multiaxial stress are presented. A concept of the surface, on which energy is dissipated at a constant rate, has been applied to the secondary creep behaviour discussion. It is shown that such a concept can be successfully applied when describing evolution of the material creep properties due to different types of plastic predeformation.

A determination procedure of experimental isochronous creep rupture surfaces basing on creep tests on pure copper is reported. The curves of the same time to rupture determined on the basis of experimental programme are compared with theoretical predictions resulted from application of the most often used creep rupture criteria. It is shown that the Sdobyrev creep rupture criterion gives the most accurate description of the experimental results.

1. Introduction

Experimental creep investigations of metals under multiaxial stress conditions have been recently regarded as one of the most important tasks of the engineering projects dealing with designing and producing many of the reliable elements of construction subjected simultaneously to high temperatures and complex loading. In general, these are structural components working in the coal and nuclear power plants, factories of the chemical industry, aeroplanes, spaceships, etc. The reason for wide dissemination of such investigations over the world is connected with the safety of the personnel employed in these industrial branches as well as any other peoples, and moreover, with the problem of natural environment protection against different kinds of pollution. Neglecting material structure degradation due to the creep process may lead

to ecological disasters which in the case of nuclear power plants can have a global character.

Experimental creep investigations under complex stress states are developing parallelly in several directions. In general, however, they can be divided into the following two groups:

- Industrial investigations
- Modelled investigations.

First of them includes usually investigations of particular elements of constructions, or alternatively, materials destined for their production. The second group contains tests the main goal of which is to develop experimental methods giving the best results under minimum cost, which than could be efficiently used in the industrial investigations. Such investigations are usually carried out at stress levels which are higher than those applied in practice. Moreover, in these tests materials more sensitive to the creep are often examined. The aim of these simplifications is to accelerate the developing process of new efficacious methods of creep investigation.

The results coming from creep tests under complex stress states often pose many difficulties either in their proper interpretation or in comparative studies. The creep surface concept simplifies significantly the creep data analysis in such investigations. However, in the literature on this subject this term can be attributed to the parameters describing different parts of the creep process, i.e., it can be used in the analysis of creep results concerning primary, secondary and tertiary stages of the process.

The creep surface concept was studied theoretically by Calladine and Drucker (1962), Rabotnov (1969) and Betten (1981). In their approaches the creep surface term is connected with the secondary creep period and denotes the surface of constant rate of energy dissipation or, alternatively, the surface of constant creep rate. Such an approach was verified experimentally for a range of engineering materials (cf Blass and Findley (1971); Brown (1970); Kowalewski (1987a,b), (1988), (1991); Mark and Findley (1978); Oytana et al. (1982)). It has been found (cf Kowalewski (1988) and (1991)) that the surface of constant rate of energy dissipation can be successfully used for a material with anisotropy induced by prior plastic deformation.

A wider application of the creep surface concept is observed in analysis of the creep to rupture tests carried out under complex stress states (cf Chrzanowski and Madej (1980); Hayhurst (1972) and (1983); Hayhurst et al. (1980); Jakowluk and Plewa (1983); Kowalewski (1996); Kowalewski et al. (1994); Leckie and Hayhurst (1977); Litewka (1989) and (1991); Litewka and

Hult (1989); Piechnik and Chrzanowski (1970); Rogalska (1990)). In this case the creep surface is usually defined as a set of points representing the same lifetime in the stress space considered.

The main aim of this paper is to report creep results from multiaxial investigations, which have been carried out in the Institute of Fundamental Technological Research during last ten years. Results of these tests are illustrated by means of the creep surface concept. In the first part the results are shown in form of the surfaces of constant rate of energy dissipation obtained on the basis of experimental procedure comprising creep tests at 573 K, the objective of which was to determine a minimum creep rate. Evolution of the initial surface of constant rate of energy dissipation due to strain induced anisotropy is also presented.

In the second part, the methods of determination of the surfaces representing the same time to rupture during the creep process are demonstrated on the basis of either theoretical considerations or creep experiments on copper at 523 K.

2. Surface of constant rate of energy dissipation describing secondary creep period

2.1. Theoretical approach

Creep deformations at the secondary stage of the process are usually large and of similar character as pure plastic deformations. Since creep deformations of metals are typically non influenced if a hydrostatic pressure is superimposed, the theory is often based on the assumption of the existence of a creep potential, which can depend only on invariants of the stress tensor or its deviator, if the material is isotropic. Certain considerations that favour the creep potential hypothesis were presented by Calladine and Drucker (1962), Rabotnov (1969), Betten (1981), Betten and Waniewski (1989).

The creep potential concept can be also used for anisotropic materials. In this case the creep potential may be represented as a polynomial in stresses which is invariant under the subgroup of transformations associated with the crystal class considered. Therefore, we must form a polynomial basis for the subgroup of transformations describing the symmetry properties of the crystal class. The creep potential is then expressible as a polynomial in these invariants, which form a functional basis (cf Betten (1981)).

The power of energy dissipation in creep can be expressed in the following general form (cf Rabotnov (1969))

$$L = \sigma_{ij} \dot{\epsilon}_{ij} \quad (2.1)$$

where

- σ_{ij} - stress tensor
 $\dot{\epsilon}_{ij}$ - strain rate tensor.

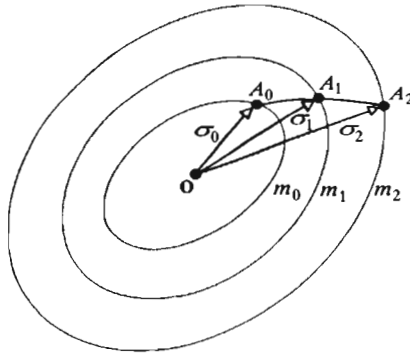


Fig. 1. Theoretical surfaces of a constant rate of energy dissipation

Assuming $L(\sigma_{ij}) = m_n = \text{const}$, the hypersurface of constant dissipation power can be obtained in the stress space. Dissipation power cannot decrease with the increase in loading, i.e., at each point on the A_0A_2 loading path, Fig.1, the following relationship is valid

$$\left(\sigma_{ij}^{(m_2)} - \sigma_{ij}^{(m_0)} \right) \dot{\epsilon}_{ij} \geq 0 \quad (2.2)$$

This condition represents a transformation of Drucker's postulate from the theory of plasticity to the theory of stationary creep. Basing on the relative maximum principle of the dissipation power increment, which arises from the theory of plasticity, the steady state creep rate can be expressed in form

$$\dot{\epsilon}_{ij}^{(\min)} = h(\sigma_{ij}) \frac{\partial L}{\partial \sigma_{ij}} \quad (2.3)$$

Now, it is easy to find a function $F(\sigma_{ij})$ called the creep rate potential (cf Rabotnov (1969))

$$h(\sigma_{ij}) \frac{\partial L}{\partial \sigma_{ij}} = \frac{\partial F(\sigma_{ij})}{\partial \sigma_{ij}} \quad (2.4)$$

From Eq (2.3) it follows

$$\dot{\varepsilon}_{ij}^{(\min)} = \frac{\partial F(\sigma_{ij})}{\partial \sigma_{ij}} \quad (2.5)$$

If L is a homogeneous stress function of $n+1$ order, then from Euler's theorem for a homogeneous function the following expressions can be obtained

$$h = \frac{1}{1+n} \quad F = \frac{1}{1+n} L \quad (2.6)$$

Additionally, assuming isotropy and incompressibility of a material the creep potential F may be expressed as a function of the second J_2 and the third J_3 invariants of the stress deviator

$$F = F(J_2, J_3) \quad (2.7)$$

Taking into account similarity of the stress and creep strain rate deviators Eq (2.7) reduces to

$$F = F(J_2) \quad (2.8)$$

Thus, for an isotropic body under plane stress conditions, i.e., stress states usually met in experiments, the initial creep surface takes the well known form

$$F = F(J_2) = \sqrt{\sigma_{11}^2 - \sigma_{11}\sigma_{22} + \sigma_{22}^2 + 3\sigma_{12}^2} = \text{const} \quad (2.9)$$

which is graphically represented in the $(\sigma_{11}, \sigma_{22}, \sigma_{12})$ stress space by the Huber-Mises ellipsoid (cf Szczepiński (1963)).

2.2. Experimental creep surfaces

The concept of the steady-state creep surfaces has been experimentally studied for aluminium alloys (cf Blass and Findley (1971); Brown (1970)), for the 304 stainless steel (cf Mark and Findley (1978)), and for the pure copper (cf Kowalewski (1987a,b), (1988) and (1991)). It has been found (cf Brown (1970)) that the shape of creep surfaces (defined as surfaces of the same secondary creep rate) at elevated temperature for an aluminium alloy under proportional loading was similar to that of the room temperature yield locus. The same phenomenon was observed for the 304 stainless steel by Mark and Findley (1978). Contrary to these results the creep surfaces obtained by Kowalewski (1988) and (1991) for the pure copper differed from the room

temperature yield surface. The creep surface in this case was determined on the basis of the assumption

$$L = \sigma_e \dot{\epsilon}_e^{(\min)} = \text{const} \quad (2.10)$$

where

$$\begin{aligned} \sigma_e & - \text{effective stress, } \sigma_e = \sqrt{(3/2)S_{ij}S_{ij}} \\ \dot{\epsilon}_e^{(\min)} & - \text{effective steady creep rate, } \dot{\epsilon}_e^{(\min)} = \sqrt{(2/3)\dot{\epsilon}_{ij}^{(\min)}\dot{\epsilon}_{ij}^{(\min)}}. \end{aligned}$$

Initial creep surface satisfying Eq (2.10) was determined on the basis of tests performed on the thin-walled specimens at three values of the effective stress: 31; 41; 45 (all of them were lower than the yield point of the material at the test temperature equal to 573 K ($R_{0.2} = 50$ MPa)). Tests were carried out under plane stress states being various combinations of an axial force and twisting moment. The stress states for each stress level were defined by the angle $\Theta_\sigma = \arctan \sqrt{3}\sigma_{12}/\sigma_{11}$, equal to 0; 30; 60; 90°. The results of this research procedure are presented in detail elsewhere (cf Kowalewski (1987a,b)), so in this paper they will be only shortly summarized. For all stress states the experimental points plotted in the logarithmic scale diagrams the normalized secondary creep rate versus of normalized stress level were located on the straight lines. The data obtained at the lowest stress level under tension were chosen as the normalization factors. Each line was attributed to a different stress state. It enabled one to describe the experimental data by a modified Norton rule (cf Kowalewski (1987a)). This modification is based on the assumption that the material parameters $\dot{\epsilon}_0$, n in Norton equation (cf Norton (1929)) may be expressed as the functions depending on the type of stress state

$$\frac{\dot{\epsilon}_e^{(\min)}}{\dot{\epsilon}_0(\Theta_\sigma)} = \left(\frac{\sigma_e}{\sigma_0}\right)^{n(\Theta_\sigma)} \quad (2.11)$$

Having diagrams of the material parameters variations versus direction determining a type of stress state and applying a modified Norton equation (2.11) the initial surfaces of constant rate of energy dissipation can be obtained from the following relation

$$\sigma_e(\Theta_\sigma) = \left[\frac{L\sigma_0^{n(\Theta_\sigma)}}{\dot{\epsilon}_0(\Theta_\sigma)} \right]^{\frac{1}{n(\Theta_\sigma)+1}} \quad (2.12)$$

The examples of creep surfaces determined in this way are presented in Fig.2. They are compared with the surfaces resulted from the potential theory for the isotropic materials, which assumes the creep potential as a function

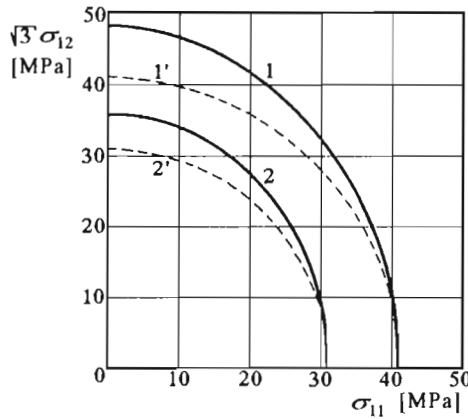


Fig. 2. Initial surfaces of a constant rate of energy dissipation for pure copper. The surfaces denoted by 1 and 1' correspond to $L = 906 \cdot 10^{-5}$ MPa/h, while the surfaces denoted by 2 and 2' correspond to $L = 155 \cdot 10^{-5}$ MPa/h (bold solid lines reflect surfaces determined on the basis of experimental data, whereas broken lines represent theoretical predictions assuming a creep potential in the form of second invariant of the stress deviator tensor)

of the second invariant of the stress deviator. Although results of the experiments for annealed copper proved the isotropic material behaviour during monotonic loading tests (yield locus pretty well satisfies the Huber-Mises condition), it demonstrated anisotropic properties under creep conditions. The tests clearly showed that the secondary creep rates at uniaxial tension creep were significantly higher than those at pure torsion creep achieved. Considering the initial creep surfaces, Fig.2, the anisotropy defined as a ratio of stress levels under the tension and torsion loadings, with L given, exceeds 12% in the case of effective stress equal to 31 MPa and 16% if $\sigma_e = 41$ MPa. Therefore, the experimental data could not be described by the surface determined with the use of the potential theory, which assumes a creep potential in the form of second invariant of the stress deviator only.

The method used to obtain the initial creep surface has been also applied to assessment of the effect of prior strain induced anisotropy on the creep behaviour and to description of evolution of the preliminary surface of constant rate of energy dissipation (cf Kowalewski (1987b), (1988) and (1991)). For all tests, each thin-walled specimen was at first proportionally deformed up to 5% of the effective plastic prestrain either by uniaxial tension (8 specimens) or by pure torsion (also 8 specimens). The experimental procedure consisted

of creep tests under the two effective stresses equal to 31 and 41 MPa. A four different types of stress states, defined by Θ_σ , were realized for each stress level. The creep surfaces for the copper subjected to prior cold work were determined on the basis of experimental data.

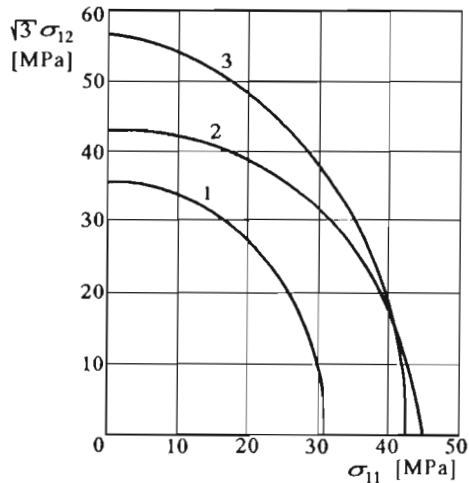


Fig. 3. Comparison of the initial surface of a constant rate of energy dissipation (1) for the virgin copper with surfaces representing the same material after plastic predeformation under uniaxial tension (2) and pure torsion (3). The surfaces have the same rate of energy dissipation ($L = 155 \cdot 10^{-5}$ MPa/h)

The evolution of creep surface is graphically illustrated by comparison of shapes and magnitudes of the locus for the virgin material and for the same material prestrained by uniaxial tension as well as pure torsion, Fig.3. These surfaces were calculated for the same value of L equal to $155 \cdot 10^{-5}$ MPa/h (which corresponds to L in the steady creep test for $\sigma_e = 31$ MPa and $\Theta_\sigma = 0^\circ$). As it can be observed from Fig.3, the magnitude of the creep surfaces for prestrained copper is markedly greater in comparison with the virgin material, and the maximum displacements of the creep surfaces are coaxial with directions of the room temperature strain induced tensor.

The experiments and theory presented so far were limited to the second stage of the creep process. Since it has been found that tertiary creep for some materials lasts longer than 50% of their lifetime, it seems to be worthwhile, from a practical point of view, to consider theory and experimental methods applied to studying this creep stage.

3. Isochronous creep rupture surfaces

3.1. Theoretical approach

It has been found that multi-axial creep rupture results are conveniently plotted in terms of isochronous surfaces (cf Chrzanowski and Madej (1980); Hayhurst (1972) and (1983); Hayhurst et al. (1980); Jakowluk and Plewa (1983); Kowalewski (1996); Kowalewski et al. (1994); Leckie and Hayhurst (1977); Litewka (1989) and (1991); Litewka and Hult (1989); Piechnik and Chrzanowski (1970); Rogalska (1990)) representing loci of constant rupture time in a stress space. Determination of the shape of these surfaces requires multi-axial creep constitutive equations. Having the uniaxial creep theory proposed by Kachanov (1958) and Rabotnov (1969) it was not possible to determine the isochronous creep rupture locus. Therefore, Leckie and Hayhurst (1977) have attempted to generalize the single state Rabotnov-Kachanov equations to multi-axial states of stress. The generalization of the uniaxial equations for multi-axial stresses has been achieved accepting the assumption that the influence of continuum damage on the deformation rate is scalar in character, and introducing the homogeneous stress function which reflects the stress state effects on the time to rupture. The way of generalization was also influenced by the experimental results of Johnson et al. (1956) and (1962) according to which the strain rates are dependent on the effective stress, and the components of strain rate tensor are proportional to the components of deviatoric stress. Leckie and Hayhurst (1977) also accepted the fact, known from Johnson's tests, that when deterioration is taking place in the tertiary region, the ratio of the strain rate components remains sensibly constant and equals to the value in the steady state portion. The equations representing multi-axial conditions can then be written as

$$\frac{\dot{\varepsilon}_{ij}}{\dot{\varepsilon}_0} = \frac{3}{2} \left(\frac{\sigma_e}{\sigma_0} \right)^{n-1} \frac{S_{ij}}{\sigma_0} \frac{1}{(1-\omega)^n} \quad (3.1)$$

$$\frac{\dot{\omega}}{\dot{\omega}_0} = \Delta^\nu \frac{1}{(1+\eta)(1-\omega)^\eta} \quad (3.2)$$

where $\dot{\varepsilon}_0$, σ_0 , $\dot{\omega}_0$, n , ν , η are constants, ω is a damage variable, $\Delta = \Delta(\sigma_{ij}/\sigma_0) = \sigma_{\max}/\sigma_0$ for copper, and $\Delta = \Delta(\sigma_{ij}/\sigma_0) = \sigma_e/\sigma_0$ for aluminium alloys. Integration of the damage evolution equation (3.2) for the following boundary conditions: $\omega = 0$, $t = 0$ and $\omega = 1$, $t = t_R$, yields after normalization the relation describing time to rupture

$$\frac{t_R}{t_0} = \frac{1}{\Delta^\nu} \quad (3.3)$$

Substitution for $t_R = t_0$ into Eq (3.3) gives the equation of the isochronous surface.

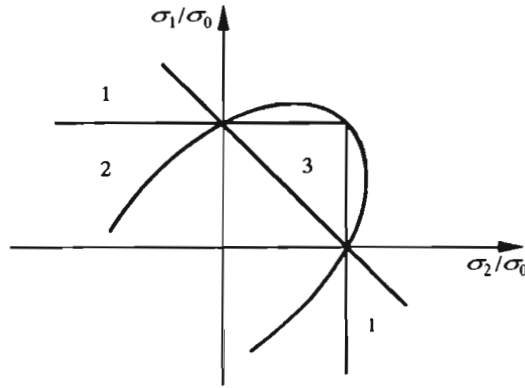


Fig. 4. Isochronous creep rupture surfaces for different rupture criteria (σ_1, σ_2 denote the principal stresses)

For the plane stress conditions, the isochronous surfaces obtained for different rupture criteria are illustrated in Fig.4. According to Johnson et al. (1956) and (1962) the rupture criteria for an aluminium alloy and pure copper appear to represent the extremes of a material behaviour since the isochronous surface for many metals lies somewhere between these criteria. In spite of the fact that these observations have been made on the basis of a relatively limited amount of the experimental data and in certain cases did not give precise description of the rupture, they are still influencing the process of new creep damage models development. Typical examples of this situation are: the rupture criterion applied by Dyson and McLean (1977), in which they assumed that the creep damage of Nimonic 80A tested at 1023 K was governed by the criterion being a product of the effective stress and maximum principal stress criteria, respectively, and the creep rupture criterion proposed by Sdobyrev (1959) in the following form

$$t_R^{(Sdob)} = A [\beta \sigma_{\max} + (1 - \beta) \sigma_e]^{-\nu} \quad (3.4)$$

where σ_e represents the effective stress defined by the second invariant of the stress deviator, σ_{\max} denotes the maximum principal stress, β denotes the coefficient, determined experimentally, reflecting a degree of dependence between time to rupture and σ_e, σ_{\max} .

On the basis of results from tests on cruciform specimens (cf Hayhurst (1972)) and Johnson's investigations (1956) and (1962) on thin-walled tubular

testpieces, Hayhurst (1972) attempted to describe the multi-axial behaviour for several materials and suggested the general relationship

$$t_R^{(\text{Hay}_1)} = f(J_1, J_2, J_3) \quad (3.5)$$

where f is a homogeneous algebraic function of stress invariants. It has been found that both the relationships given by Eqs (3.4) and (3.5) can represent accurately the behaviour of copper alloys in the tension-compression quadrant of the diagram in Fig.4 but the predictions of rupture time are in error for biaxial tension stresses. The biaxial tension stress levels predicted by Eqs (3.4) and (3.5) are too high and too low, respectively. On the basis of these remarks, Hayhurst (1972) has proposed the criterion which is capable to express the different types of behaviour represented by the Eqs (3.4) and (3.5)

$$t_R^{(\text{Hay}_2)} = A \left[a\sigma_{\max} + bJ_1 + c\sqrt{J_2'} \right]^{-\nu} \quad (3.6)$$

being a linear combination of the maximum principal tensile stress and the first and second stress invariants, where

- A, ν - material constants, independent of stress
- a, b, c - constants
- J_1, J_2' - first invariant of stress tensor and second invariant of stress deviator, respectively.

In Eq (3.6) a, b, c are constants, with $a + b + c = 1$, limiting the influence of particular terms in the criterion (3.6) on the time to rupture. By selecting appropriate values of these constants, all the simple rupture criteria previously discussed can be represented, i.e.:

- (I) The maximum principal stress rupture criterion, if $a = 1, b = c = 0$; its graphical interpretation for the biaxial stress state is represented by the two straight lines (1), Fig.4
- (II) The Huber-Mises effective stress criterion, if $c = 1, a = b = 0$, represented by the ellipse (2) in Fig.4
- (III) The maximum hydrostatic stress criterion defined by the first invariant of the stress tensor, if $b = 1, a = c = 0$, represented by the straight line (3) in Fig.4.

The simple creep rupture criteria presented in graphical form in Fig.4 do not cover an influence of stress level on the shape of isochronous curves. However, the analyses of experimental data from biaxial creep rupture tests for different metals prove that the size as well as the shape of the isochronous

creep rupture curve depend on the stress level (cf Finnie and Abo el Ata (1971); Litewka (1989) and (1991); Litewka and Hult (1989)). For the low stress level tests the creep rupture depends mainly on the magnitude of the maximum principal stress, while at higher stress levels the rupture criterion often seems to be the Huber-Mises effective stress. In other words, the shape of isochronous curves changes when the stress level is increased from a more pointed (represented by lines 1 in Fig.4) to a more rounded shape (represented by curve 2 in Fig.4).

3.2. Experimental approach

The paper summarizes the approach proposed by Kowalewski (1996) in order to determine surfaces of the same time to rupture on the basis of creep tests carried out on pure copper under the plane stress state at elevated temperature. Creep investigations were carried out on the thin-walled tubular testpieces of 22 mm internal diameter, 1.5 mm wall thickness, and 40 mm gauge length with the use of biaxial creep testing machine which enabled realization of plane stress conditions at elevated temperature (523 K).

The experimental procedure consisted of creep tests up to rupture for copper specimens subjected to various combinations of an axial force and twisting moment necessary for three different values of effective stress ($\sigma_e = 70.0; 72.5; 75.0$ MPa), defined in the same way as in the procedure used to determine minimum creep rates described in the previous section. Creep tests were carried out under tension ($\Theta_\sigma = \arctan \sqrt{3}\sigma_{12}/\sigma_{11} = 0^\circ$), torsion ($\Theta_\sigma = 90^\circ$) and combination of these loadings ($\Theta_\sigma = 45^\circ$). Prior to creep test each specimen was heated uniformly at the test temperature (523 K) for 24 hours. All creep tests were carried out at stress levels lower than the yield point of the material at 523 K ($R_{0.2} = 76$ MPa).

The results of creep to rupture tests have been discussed in detail elsewhere (cf Kowalewski (1995)).

The creep parameters, e.g., minimum creep rate, time to rupture, duration of typical creep periods, characterising macroscopically creep behaviour prove that the process is sensitive to a stress state, in spite of the initial isotropy of material in the sense of such parameters as Young's modulus, yield limit or ultimate tensile stress.

As it was mentioned previously, the useful graphical representation of biaxial creep rupture data is offered by isochronous loci. Experimental determination of the isochronous surface requires many creep tests at various stress

states and at several stress levels. For anisotropic materials it is difficult to determine experimentally such a surface with sufficient accuracy. However, it can be done with a relatively good approximation using the relationship $\log(\sigma_e) = f[\log(t_R)]$, Fig.5. In this figure the results for three types of stress states are presented. Data points for a chosen type of stress state with a relatively high accuracy are located on the straight lines which have different positions. These lines were obtained with the use of least squares technique. Taking into account as a reference point the line representing pure torsion results the remaining straight lines are shifted and rotated. Analysis of the positions of these lines indicates that the material subjected to the creep process under uni-axial tension is significantly more sensitive to stress variations in comparison with the same material tested either at pure torsion or a combination of tension and torsion. On the basis of the fitted lines, shown in Fig.5 (bold solid lines), drawing straight lines parallel to the vertical axis (stress axis) with the objective to intersect the approximate lines representing experimental data, it is easy to determine the points connecting the same times to rupture.

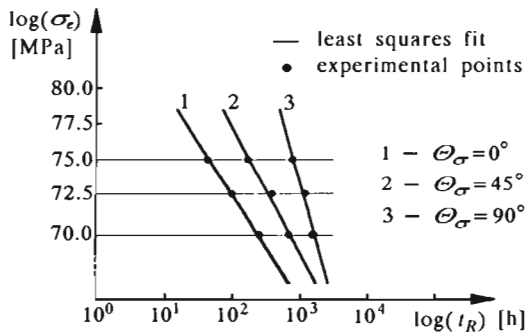


Fig. 5. Logarithmic diagram of the relation $\log(\sigma_e) = f[\log(t_R)]$ for the considered stress states

The points of intersection of vertical line for the rupture time taken into account with the approximate lines provide the values of effective stress necessary for attaining the rupture at a particular type of stress state. These values can be approximated at the stress plane $(\sigma_{11}, \sqrt{3}\sigma_{12})$ and, as a consequence, the isochronous curves are determined. The surfaces of the same lifetime for the rupture time equal to 400, and 1000 h are shown in Fig.6. The surface corresponding to the rupture time equal to 400 h has been selected for further comparative studies presented in the next section.

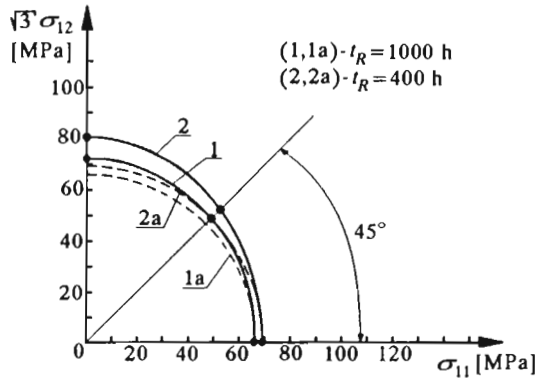


Fig. 6. Comparison of the isochronous creep rupture surfaces, $t_R = 400; 1000$ h, determined on the basis of experimental results (solid lines) with the theoretical surfaces calculated from the Huber-Mises effective stress rupture criterion (dashed lines)

3.3. Comparison of the isochronous creep rupture surfaces

The curve of the same time to rupture determined on the basis of experimental procedure is compared with theoretical predictions from the following creep rupture hypotheses:

- The maximum principal stress rupture criterion, which is defined in the stress co-ordinate system $(\sigma_{11}, \sigma_{12})$ corresponding to the experimental procedure by the following relationship

$$\sigma_R = \sigma_{\max} = \frac{1}{2} \left(\sigma_{11} + \sqrt{\sigma_{11}^2 + 4\sigma_{12}^2} \right) \quad (3.7)$$

- The Huber-Mises effective stress rupture criterion, which for the combination of stresses used in experiments takes the form

$$\sigma_R = \sigma_e = \sqrt{\sigma_{11}^2 + 3\sigma_{12}^2} \quad (3.8)$$

- The Sdobyrev creep rupture criterion (cf Sdobyrev (1959)) given by

$$\sigma_R = \beta\sigma_{\max} + (1 - \beta)\sigma_e \quad (3.9)$$

The isochronous surfaces resulting from these rupture criteria are compared to the surface determined on the basis of experimental results, Fig.7.

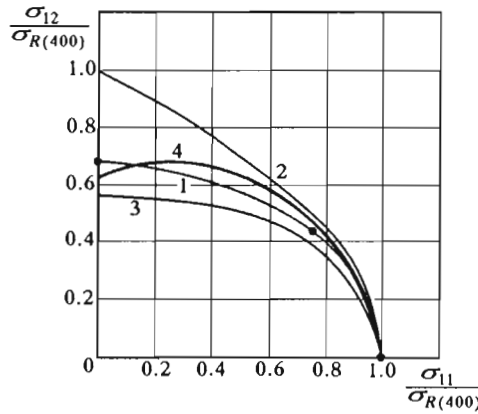


Fig. 7. Comparison of the isochronous creep rupture surface determined on the basis of experimental results (1) for $t_R = 400$ h with the surfaces calculated for the same rupture time according to: (2) - the maximum principal stress rupture criterion, (3) - the Huber-Mises effective stress rupture criterion, and (4) - the Sdobyrev creep rupture criterion. Normalization of the co-ordinate system is carried out with the use of the reference tension stress giving the time to rupture of 400 h

All the curves are presented in the normalized co-ordinate system and refer to the rupture time equal to 400 h. Tension stress corresponding to the lifetime of 400 h has been selected as the normalization factor ($\sigma_{R(400)}$). As it is clearly shown, the best description of the experimental data is achieved for the Sdobyrev creep rupture criterion taken with the coefficient $\beta = 0.9$ calculated on the basis of creep tests carried out. The value of β indicates that the damage mechanism governed by the maximum principal stress, played significant role in the creep rupture of the copper tested. Hence, this result can be treated as the confirmation of the earlier observed creep behaviour of the copper having similar chemical composition (cf Hayhurst (1972) and (1983); Johnson et al. (1956) and (1962)).

4. Conclusions

- Theoretical and experimental methods of the multiaxial creep data analysis were studied. It was shown that a discussion of the results in terms of the creep surface concept provides main information on the material behaviour in a very convenient and concise form enabling their further simple application by engineers.

- Results of the secondary creep for both the virgin and prestrained copper can be successfully analysed on the basis of the surface of constant rate of energy dissipation.
- It was shown that such a surface for the virgin copper is not of the same shape as the room temperature yield locus.
- It was found that room temperature plastic predeformation caused the increase of the creep resistance of copper at 573 K expressed by a considerable decrease in the secondary creep rate.
- For the tested material the parameters which characterise creep process such as, duration of primary creep period, steady creep rate, time to rupture and ductility were functions of the type of stress state.
- A methodology for convenient determination of the isochronous creep rupture surfaces on the basis of biaxial tests was reported.
- Verification of the fundamental creep rupture criteria exhibited that the Sdobyrev criterion gives the most promising tool enabling description of the damage process of the copper under the long-term constant loading conditions at elevated temperature.

References

1. BETTEN J., 1981, Representation of Constitutive Equations in Creep Mechanics of Isotropic and Anisotropic Materials, *Proc. of 3rd IUTAM Symp. "Creep in Structures"*, Edit. A.R.S. Ponter and D.R. Hayhurst, Springer-Verlag, Berlin Heidelberg, 179-201
2. BETTEN J., WANIEWSKI M., 1989, Multiaxial Secondary Creep Behaviour of Anisotropic Materials, *Archives of Mechanics*, **41**, 5, 679-695
3. BLASS J., FINDLEY W.N., 1971, Short Time, Biaxial Creep of an Aluminium Alloy with Abrupt Changes of Temperature and State of Stress, *ASME J. Appl. Mech.*, **38**, 489
4. BROWN G.M., 1970, Inelastic Deformation of an Aluminium Alloy under Combined Stress at Elevated Temperature, *J. Mech. Phys. Sol.*, **18**, 383
5. CALLADINE C.R., DRUCKER D.C., 1962, Nesting Surfaces of Constant Rate of Energy Dissipation in Creep, *Q. Appl. Math.*, **20**, 79
6. CHRZANOWSKI M., MADEJ J., 1980, The Construction of Failure Limit Curves By Means of a Damage (in Polish), *Theoretical and Applied Mechanics*, **18**, 4, 587-601

7. DYSON B.F., MCLEAN D., 1977, Creep of Nimonic 80A in Torsion and Tension, *Metal Sci.*, **11**, 2, 37-45
8. FINNIE I., ABO EL ATA M.M., 1971, Creep and Creep-Rupture of Copper Tubes under Multiaxial Stress, *Advances in Creep Design*, Edit. A.J. Smith, A.M. Nicolson, J. Willey, New York, 329-352
9. HAYHURST D.R., 1972, Creep Rupture under Multi-Axial States of Stress, *J. Mech. Phys. Solids*, **20**, 381-390
10. HAYHURST D.R., 1983, On the Role of Creep Continuum Damage in Structural Mechanics, *Engineering Approaches to High Temperature Design*, Edit. Wilshire B., Owen D.R.J., Pineridge Press, Swansea, 85-176
11. HAYHURST D.R., TRAMPCZYŃSKI W.A., LECKIE F.A., 1980, Creep Rupture under Non-Proportional Loading, *Acta Metallurgica*, **28**, 1171-1183
12. JAKOWLUK A., PLEWA M., 1983, Investigations of Vibrocreep Strength of the Grey Cast Iron at Complex Stress States (in Polish), *Proc. of I Symp. on Creep Problems of Materials*, Bialystok, 305-316
13. JOHNSON A.E., HENDERSON J., MATHUR, V.D., 1956, Combined Stress Fracture of Commercial Copper at 250°C, *The Engineer*, **202**, 261
14. JOHNSON A.E., HENDERSON J., KHAN B., 1962, *Complex-Stress Creep, Relaxation and Fracture of Metallic Alloys*, H.M.S.O., Edinburgh
15. KACHANOV L.M., 1958, *The Theory of Creep* (English Translation Edited By Kennedy A.J.), National Lending Library, Boston Spa
16. KOWALEWSKI Z., 1987a, The Surface of Constant Rate of Energy Dissipation under Creep and its Experimental Determination, *Archives of Mechanics*, **39**, 445-459
17. KOWALEWSKI Z., 1987b, The Influence of Plastic Anisotropy on the Creep of Metals under Complex Stress States (in Polish), *IFTR Reports*, **36**
18. KOWALEWSKI Z., 1988, Secondary Creep Surface and its Evolution Influenced By Room Temperature Plastic Deformation, *Proc. of Mecamat - "International Seminar on the Inelastic Behaviour of Solids: Models and Utilization"*, Besancon, France, CNRS, 1/53-64
19. KOWALEWSKI Z., 1991, Creep Behavior of Copper under Plane Stress State, *International Journal of Plasticity*, **7**, 387-404
20. KOWALEWSKI Z.L., 1995, Experimental Evaluation of the Influence of Stress State Type on Creep Characteristics of Copper at 523 K, *Archives of Mechanics*, **47**, 13-26
21. KOWALEWSKI Z.L., 1996, Biaxial Creep Study of Copper on the Basis of Isochronous Creep Surfaces, *Archives of Mechanics*, (in Press)
22. KOWALEWSKI Z.L., HAYHURST D.R., DYSON B.F., 1994, Mechanisms-Based Creep Constitutive Equations for an Aluminium Alloy, *J. Strain Analysis*, **29**, 309-316
23. LECKIE F.A., HAYHURST D.R., 1977, Constitutive Equations for Creep Rupture, *Acta Metallurgica*, **25**, 1059-1070
24. LITEWKA A., 1989, Creep Rupture of Metals under Multi-Axial State of Stress, *Archives of Mechanics*, **41**, 3-23

25. LITEWKA A., 1991, *Damage and Failure of Metals under Creep Conditions* (in Polish), Edited By Technical University of Poznań
26. LITEWKA A., HULT J., 1989, One Parameter CDM Model for Creep Rupture Prediction, *Eur. J. Mech., A/Solids*, **8**, 3, 185-200
27. MARK R., FINDLEY W.N., 1978, Concerning a Creep Surface Derived From a Multiple Integral Representation for 304 Stainless Steel under Combined Tension and Torsion, *J. Appl. Mech.*, **45**, 773
28. NORTON F.H., 1929, *Creep of Steel at High Temperatures*, McGraw-Hill, New York
29. OYTANA C., DELOBELLE P., MERMET A., 1982, Constitutive Equations Study in Biaxial Stress Experiments, *J. Engng. Mat. Tech.*, **104**, 1
30. PIECHNIK S., CHRZANOWSKI M., 1970, Time of Total Creep Rupture of a Beam under Combined Tension Bending, *Inst. J. Solids Structures*, **6**, 453-477
31. RABOTNOV Y.N., 1969, *Creep Problems in Structural Members*, North Holland Publishing Company, Amsterdam
32. ROGALSKA E., 1990, Isochronous Creep Rupture Curves, *Engineering Transactions*, **38**, 2, 295-306
33. SDOBYREV V.P., 1959, Creep Criterion for Some High-Temperature Alloys in Complex Stress State (in Russian), *Izv. AN SSSR. Mekh. and Mashinostr.*, **6**, 12-19
34. SZCZEPIŃSKI W., 1963, On the Effect of Plastic Deformation on Yield Condition, *Archives of Mechanics*, **15**, 2, 275-296

Doświadczalne badania pełzania metali w warunkach złożonego stanu naprężenia

Streszczenie

W pracy przedstawiono teoretyczne i doświadczalne metody analizowania wyników procesu pełzania metali poddawanych wieloosiowym stanom naprężenia. Wyniki dla drugiego okresu pełzania są dyskutowane za pomocą koncepcji powierzchni stałej prędkości dyssypacji energii. Pokazano, że sposób ten może być efektywnie wykorzystywany do opisu ewolucji właściwości materialu poddanego różnym typom wstępnej deformacji plastycznej.

W pracy referowana jest procedura określania izochronicznych powierzchni zniszczenia przy pełzaniu na podstawie testów pełzania wykonanych na czystej miedzi. Doświadczalnie uzyskana powierzchnia jednakowego czasu do zniszczenia porównywana jest z powierzchniami teoretycznymi wyznaczonymi dla kilku wybranych kryteriów zniszczenia w warunkach pełzania. Pokazano, że kryterium Sdobyreva najdokładniej opisuje rezultaty doświadczalne.